

Boron Nitride Dispersed Nanocomposites with High Thermal Shock Resistance

T. Kusunose, T. Sekino, Y. H. Choa*, T. Nakayama and K. Niihara

Institute of Scientific and Industrial Research, Osaka University, Osaka 567-0047, Japan

**Division of New Materials Engineering, Chonbuk National University, Chonbuk 561-756, Korea*

(Received August 24, 2001)

Abstract The microstructure and mechanical properties of $\text{Si}_3\text{N}_4/\text{BN}$ nanocomposites synthesized by chemical processing were investigated. The nanocomposites containing 15 vol% hexagonal BN (h-BN) were fabricated by hot-pressing $\alpha\text{-Si}_3\text{N}_4$ powders covered with turbostratic BN (t-BN). The t-BN coating on $\alpha\text{-Si}_3\text{N}_4$ particles was prepared by heating $\alpha\text{-Si}_3\text{N}_4$ particles covered with a mixture of boric acid and urea in hydrogen gas. TEM observations of this nanocomposite revealed that nano-sized h-BN particles were homogeneously dispersed within Si_3N_4 grains as well as at grain boundaries. The strength and thermal shock resistance were significantly improved in comparison with the $\text{Si}_3\text{N}_4/\text{BN}$ microcomposites.

Keywords : Nanocomposite, $\text{Si}_3\text{N}_4/\text{BN}$, Powder synthesis, Thermal shock resistance

1. Introduction

Silicon nitride (Si_3N_4) based ceramics have been widely used as high-temperature structural materials because of their superior mechanical and thermal properties. To extend the use of Si_3N_4 into the much wider range of high-temperatures engineering, however, further improvement in thermal shock resistance as well as machinability and corrosion resistance to molten metals is required. In order to improve these disadvantageous properties, the dispersion of hexagonal BN (h-BN) particles as a second phase in the Si_3N_4 matrix was studied.^{1,2)} But the remarkable decrease in fracture strength with an increase in BN content was observed.³⁾

Recently, Niihara and his colleagues⁴⁻⁸⁾ have investigated ceramic-based nanocomposites, in which the nano-sized particles are dispersed within the matrix grains and/or at the grain boundaries. These nanocomposites showed the improved fracture strength and excellent creep resistance compared with the monolithic ceramics. In early nanocomposite, hard and strong materials as dispersoids were mainly incorporated into the matrix. But in the several years, soft and weak materials like a metal were also used as dispersoids, and the remarkable enhancement of fracture strength was found by the addition of soft and weak dispersoids.^{9,10)} However, it has not been reported the improvement of mechanical properties by nano-sized

soft and weak ceramic dispersoid such as h-BN.

The purpose of this study is to fabricate the $\text{Si}_3\text{N}_4/\text{BN}$ nanocomposite, in which the nano-sized BN particles are homogeneously dispersed within the Si_3N_4 matrix grains and/or at the grain boundaries, by a new chemical process, and to improve the properties, especially fracture strength and thermal shock resistance.

2. Experimental Procedure

2.1. Preparation

It is difficult to homogeneously disperse fine h-BN particles by using the conventional method that involves the mixing of the commercial powders to produce composite materials. Thus, we proposed an excellent method for precipitating t-BN precursor, which is soluble in any solvent and it readily forms h-BN on the $\alpha\text{-Si}_3\text{N}_4$ particles. Boric acid is very suitable as a boron source of h-BN as previously described. Various synthesis methods for h-BN using boric acid such as direct nitridation with ammonia gas and reaction with nitrogen compound have been reported.¹¹⁻¹³⁾ In this study, the reduction method¹¹⁾ using urea as nitrogen source was chosen, because urea is harmless and soluble in various solvents and it gives little impurity after the synthesis of h-BN.

The content of BN produced by the reaction of boric acid with urea in hot-pressed sample was calculated

and adjusted to 15 vol%. For comparison, the commercial BN powders with average grain size of 9 μm were also used to fabricate $\text{Si}_3\text{N}_4/\text{BN}$ microcomposites. The $\alpha\text{-Si}_3\text{N}_4$ powder was ball milled with boric acid and urea in a plastic bottle using Si_3N_4 balls and ethanol. Before drying, 100 cm^3 of ion-exchanged water was added to the slurry to prevent the boric acid from evaporating. The dried mixtures were reduced at 1100°C for 10 h in hydrogen gas, and then heated at 1500°C for 8 h in nitrogen gas to produce the $\text{Si}_3\text{N}_4\text{-BN}$ composite powder. The composite powders were hot-pressed at 1800°C for 1 h in nitrogen gas after the second step of ball-milling with the sintering aid (2 wt% Al_2O_3 + 6 wt% Y_2O_3) and drying.

2.2. Characterization

The crystalline phases of the hot-pressed bodies and powders were determined by X-ray diffraction analysis (XRD). The microstructure was observed by a scanning electron microscope (SEM) and a transmission electron microscope (TEM). The microchemical analysis was done using an energy dispersive X-ray (EDX) analyzer attached to TEM. Grain size distribution was analyzed from SEM photographs of sections polished and subsequently etched in molten NaOH by using image analysis technique (LA-500, Pias, Ltd., Tokyo, Japan).

Bulk density was measured by the Archimedes immersion technique in toluene. Young's modulus was determined by the resonance vibration method with first-mode resonance. Fracture strength was evaluated by a three-point bending test using rectangular bars (3 \times 4 \times 37 mm). The tensile surfaces of specimens were perpendicular to the hot-pressing direction. The span length and crosshead speed were 30 mm and 0.5 mm/min, respectively. Thermal shock fracture resistance was determined by measuring the bending strength of water-quenched samples. The samples were soaked for 10 min at a selected temperature in a vertical tube furnace and then dropped into a water bath at 20°C.

3. Results and Discussion

3.1. Fabrication of $\text{Si}_3\text{N}_4/\text{BN}$ nanocomposite.

Figure 1 illustrates the transformation of crystalline phases in the $\text{Si}_3\text{N}_4/\text{BN}$ composite fabricated by the chemical route using boric acid and urea. Since the starting powder before H_2 reduction was consisted of $\alpha\text{-Si}_3\text{N}_4$, boric acid and urea, it was thought that the precipitated boric acid and urea on $\alpha\text{-Si}_3\text{N}_4$ powders did not react during the slurry drying. The reduced

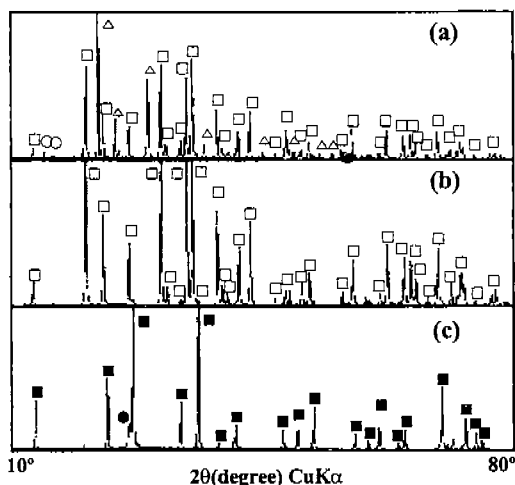


Fig. 1. XRD patterns of the $\text{Si}_3\text{N}_4/15$ vol% BN composite synthesized by the chemical route. (a) before reduction, (b) reduced at 1100°C for 10 h in H_2 and heated at 1500°C for 8 h in N_2 and (c) hot-pressed at 1800°C for 1 h in N_2 . □: $\alpha\text{-Si}_3\text{N}_4$, ■: $\beta\text{-Si}_3\text{N}_4$, ○: boric acid, ●: h-BN, △: urea.

powder revealed the almost same XRD peak as the starting powder except for the disappearance of those of boric acid and urea with the appearance of the broad peak arising from t-BN. This agrees with the XRD data for mixtures consisting of only boric acid and urea reduced by H_2 under the same conditions.

Figure 2 shows the representative TEM pictures of the reduced powder corresponding to (b) in Fig. 1. It can be observed that the $\alpha\text{-Si}_3\text{N}_4$ particles are surrounded with a low contrast phase. Based on the observation of disordered layer using higher resolution of TEM and the identification of boron using EDX, it was found that the reduced powder was $\alpha\text{-Si}_3\text{N}_4$ powders partly covered with t-BN. It is well known that turbostratic-BN (t-BN) is transformed into h-BN,^{14,15} analogous to the structure change of graphite at 2000°C in nitrogen. Actually, the broad peak of t-BN at around 25° (2θ) was developed into the peak of (002) reflection of h-BN at 26° (2θ) during hot-pressing the reduced powder at 1800°C for 1 h in nitrogen gas.

The observed sample could be identified as a composite consisting of $\beta\text{-Si}_3\text{N}_4$ and h-BN. Fig. 3 shows the TEM observation of the hot-pressed $\text{Si}_3\text{N}_4/15$ vol% BN composite from the chemical route. The nano-sized BN particles were homogeneously dispersed within Si_3N_4 grains as well as at grain boundaries. The apparent impurity phases were not observed at the interphase between Si_3N_4 and intragranular BN deve-

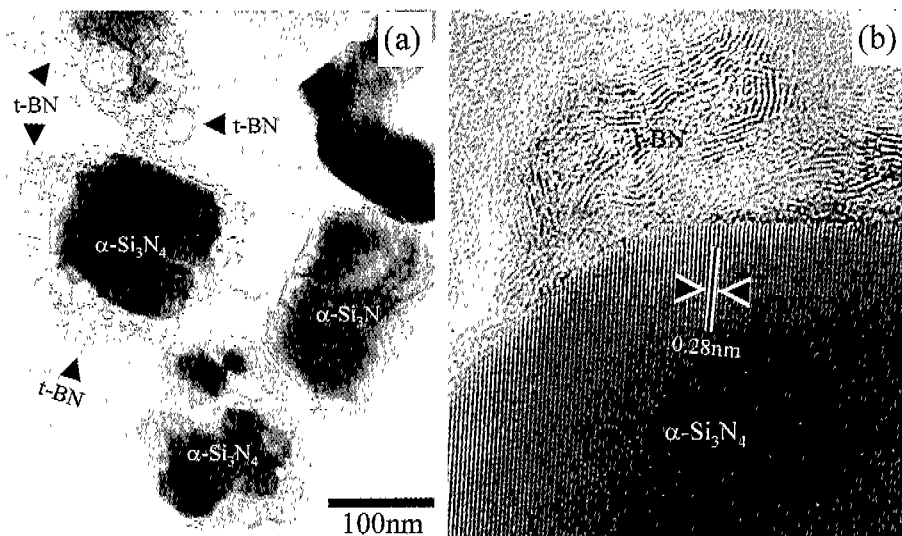


Fig. 2. TEM micrographs of t-BN formed on the surface of Si_3N_4 powder reduced in H_2 . (a) low magnification and (b) higher magnification.

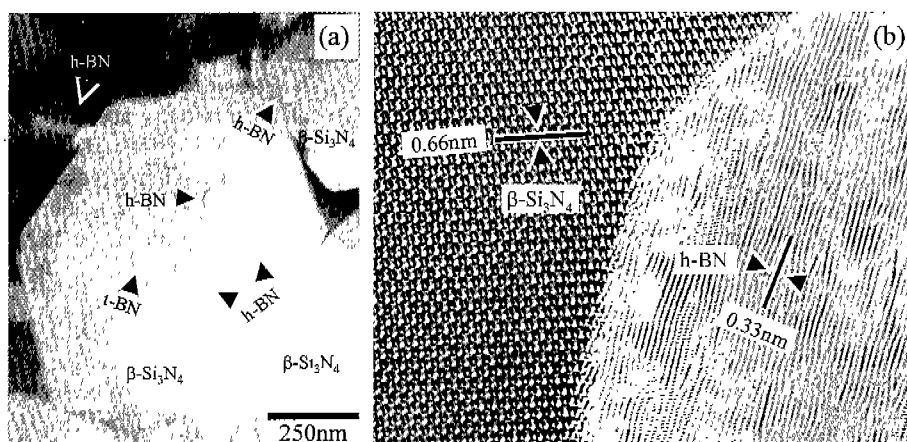


Fig. 3. TEM micrographs of $\text{Si}_3\text{N}_4/\text{BN}$ nanocomposites. (a) low magnification and (b) higher magnification of intragranular h-BN dispersion.

loped to graphite-like structure, as shown in Fig. 3(b). Now it is concluded that, $\text{Si}_3\text{N}_4/\text{BN}$ nanocomposites were successfully fabricated through a chemical process, followed by reduction and hot-pressing.

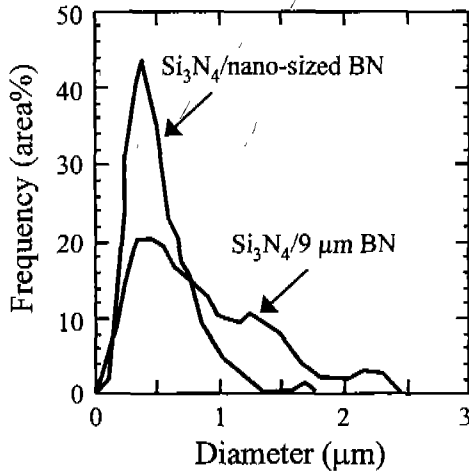
3.2. Mechanical properties

Table 1 shows Young's modulus and fracture strength of $\text{Si}_3\text{N}_4/\text{BN}$ composites. In comparison with the conventional microcomposites with the strength decreases by h-BN addition up to 15 vol%, the nanocomposites in this work were successful in retaining relatively high strength in spite of decreasing in

Young's modulus due to the soft h-BN (Young's modulus of h-BN is about 65 GPa) addition. To increase the strength of ceramics, it is necessary to increase the fracture toughness and/or to suppress the processing defects as small as possible. SEM observation of fracture surfaces showed that the fracture origin in the nanocomposites was too small to identify, while large h-BN particles or aggregations of them initiated fracture in the microcomposites. The grain size distributions of the samples, furthermore, revealed that the matrix grain size of the nanocomposites was considerably refined in comparison with the monolithic Si_3N_4 and the micro-

Table 1. Mechanical properties of $\text{Si}_3\text{N}_4/9\ \mu\text{m}$ BN and nano BN composites.

Material	$\text{Si}_3\text{N}_4/9\ \mu\text{m}$ BN	$\text{Si}_3\text{N}_4/\text{nano}$ BN
Young's Modulus (GPa)	261	262
Fracture Strength (MPa)	644	1250

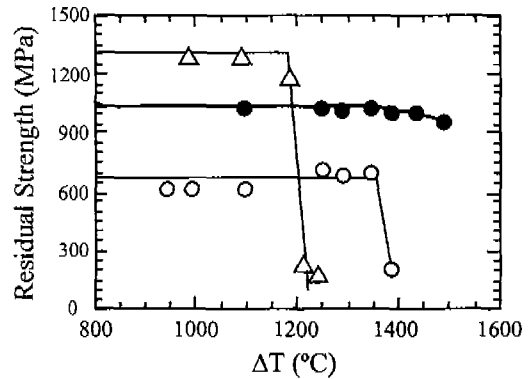

Fig. 4. Effect of BN grain size on matrix grain size distribution of $\text{Si}_3\text{N}_4/15\ \text{vol}\%$ BN composites.

composites, as shown in Fig. 4, due to inhibition of the grain growth of Si_3N_4 by the grain boundary pinning effect with nano-sized h-BN particles. Thus, relatively high strength observed for the $\text{Si}_3\text{N}_4/\text{BN}$ nanocomposites was mainly attributed to the reduction of fracture origin size and the inhibition of grain growth.

As described above, the nanocomposites fabricated in this work exhibit relatively high strength despite of BN dispersions with significantly low Young's modulus. Therefore, the remarkable improvement of thermal shock fracture resistance is expected for this nanocomposite system. Fig. 5 shows the variation of residual strength after water quenching with the temperature difference (ΔT). The residual strength of the monolithic Si_3N_4 and 15 vol% h-BN microcomposite decreased greatly at ΔT of 1200 and 1350°C, respectively, whereas the 15 vol% h-BN nanocomposite did not show the sudden decrease in strength even at 1500°C. A general and simple approach to estimate the thermal shock fracture resistance of ceramic materials is given by following equation¹⁵⁾:

$$\Delta T = \sigma(1-\nu)/E\alpha \quad (1)$$

where ΔT is the temperature difference above at


Fig. 5. Residual strength of monolithic Si_3N_4 and $\text{Si}_3\text{N}_4/\text{BN}$ composites after water-quenching as a function of temperature difference, ΔT (Δ : monolithic Si_3N_4 , \bullet : $\text{Si}_3\text{N}_4/15\ \text{vol}\%$ BN nanocomposite and \circ : $\text{Si}_3\text{N}_4/15\ \text{vol}\%$ BN microcomposites).
Table 2. Thermal expansivity of monolithic Si_3N_4 and $\text{Si}_3\text{N}_4/15\ \text{vol}\%$ BN composites.

Material	Si_3N_4	$\text{Si}_3\text{N}_4/9\ \mu\text{m}$ BN	$\text{Si}_3\text{N}_4/\text{nano}$ BN
$\alpha^*(10^{-6}/^\circ\text{C})$	3.5	3.4	3.4

*Coefficient of thermal expansion

which the residual strength decreases suddenly, σ is the strength, ν is Poisson's ratio, E is Young's modulus and α is the thermal expansion coefficient of the material. As seen in this figure, the thermal shock fracture resistance of the $\text{Si}_3\text{N}_4/\text{BN}$ nanocomposites was strongly improved compared with the microcomposites. Table 2 shows the coefficient of thermal expansion.

Considering the physical properties related to the equation (1), the improvement of the thermal shock fracture resistance for the nanocomposites is mainly attributed to the higher strength and lower Young's modulus caused by the dispersion of soft BN.

4. Conclusion

The $\text{Si}_3\text{N}_4/\text{BN}$ nanocomposites fabricated by chemical route exhibited a microstructure which consisted of nano-sized h-BN particles homogeneously dispersed within the Si_3N_4 grain as well as at the grain boundaries. As a result, Young's modulus of both conventional and nanocomposites decreased with increasing h-BN content, but the strength of the nanocomposites was significantly improved, compared with the conventional microcomposites. The enhancement of the fracture strength was attributed to the inhibition of grain growth

and the decrease in size of fracture origin. Moreover, the thermal shock fracture resistance of the $\text{Si}_3\text{N}_4/\text{BN}$ nanocomposites was significantly improved in comparison with the microcomposites. The improvement of the thermal shock resistance was mainly attributed to the high fracture strength and low Young's modulus.

Acknowledgement. This work was partly supported by a grant of the New Energy and Industrial Technology Development Organization (NEDO) and Hosokawa Powder Technology Foundation.

References

1. K. S. Mazdiyami and Robert Ruh: J. Am. Ceram. Soc., **64** (1981) 415.
2. T. Funabashi, K. Isomura, A. Harita and R. Uchimura: Ceramic Materials & Components for Engines, (1986) 986.
3. D. Goeuriot-Launay, G. Brayet and F. Thevenot: J. Mater. Sci. Lett., **5** (1986) 940.
4. K. Niihara: J. Ceram. Soc. Japan, **100** (1991) 974.
5. F. Wakai, Y. Kodama, S. Sakaguchi, N. Murayama, K. Izaki and K. Niihara: Nature, **344** (1990) 421.
6. K. Niihara: J. Jpan. Powd. and Powd. Metal., **37** (1990) 348.
7. K. Niihara, K. Izaki and A. Nakahira: J. Jpan. Powd. and Powd. Metal., **37** (1990) 352.
8. K. Niihara and T. Hirai: Ceramics, **21** (1986) 598.
9. T. Sekino, T. Nakajima, S. Ueda and K. Niihara: J. Am. Ceram. Soc., **80** (1997) 1139.
10. T. Sekino and K. Niihara: J. Mater. Sci., **32** (1997) 3943.
11. T. E. O'Connor: J. Am. Chem. Soc., **84** (1962) 415.
12. R. T. Paine and C. K. Narula: Chem. Rev., **90** (1990) 73.
13. T. Hagio, K. Kobayashi and T. Sato: J. Ceram. Soc. Japan, **102** (1994) 1051.
14. W. Sinclair and H. Simmons: J. Mater. Sci. Lett., **6** (1987) 627.
15. D. P. H. Hasselman: Am. Ceram. Soc. Bull., **49** (1970) 1033.